Computer Communications 193 (2022) 94–108

Contents lists available at ScienceDirect

Computer Communications

journal homepage: www.elsevier.com/locate/comcom

Deployment of UAV-mounted Access Points for VoWiFi Service with guaranteed QoS

Vicente Mayor, Rafael Estepa *, Antonio Estepa *, Germán Madinabeitia

Department of Telematics Engineering, Universidad de Sevilla, Spain

ARTICLE INFO

Keywords:
Unmanned Aerial Vehicle (UAV)
Wireless LAN
Voice over IP (VoIP)
Quality of Service (QoS)

ABSTRACT

Unmanned Aerial Vehicle (UAV) networks have emerged as a promising means to provide wireless coverage in open geographical areas. Nevertheless, in wireless networks such as WiFi, signal coverage alone is insufficient to guarantee that network performance meets the quality of service (QoS) requirements of real-time communication services, as it also depends on the traffic load produced by ground users sharing the medium access.

We formulate a new problem for UAVs optimal deployment in which the QoS level is guaranteed for real-time voice over WiFi (VoWiFi) communications. More specifically, our goal is to dispatch the minimum number of UAVs possible to provide VoWiFi service to a set of ground users subject to coverage, call-blocking probability, and QoS constraints. Optimal solutions are found using well-known heuristics that include K-means clusterization and genetic algorithms. Via numerical results, we show that the WiFi standard revision (e.g. IEEE 802.11a/b/g/n/ac) in use plays an important role in both coverage and QoS performance and hence, in the number of UAVs required to provide the service.

1. Introduction

The past decade has seen tremendous growth in the use of unmanned aerial vehicles (UAVs). UAVs, or so-called drones, have attracted significant interest for numerous applications in the context of smart cities, collection and dissemination of information, search and rescue, or agriculture, just to name a few [1].

There is increasingly more research focused on the deployment of UAVs for providing fast and temporal wireless communication infrastructure [2,3]. A typical UAV-assisted communication example is the provision of reliable connectivity between clustered non-directly communicated users [4] (UAV-aided communication relays). Other applications include the deployment of quasi-stationary UAV-mounted base stations to create a communication service, deploying emergency infrastructure in disaster scenarios [5–7], reaching remote areas that could not be serviced otherwise [8], or offloading existing base stations [9]. In the aforementioned applications, optimal drone location problems typically minimize the number of drones deployed (i.e. cost) to provide coverage to a set of ground users in known positions [10].

UAV optimal deployment problems generally assume that coverage (i.e. received signal strength) suffices for the provision of communication services [11]. Nevertheless, although this may hold for cellular networks (which include mechanisms to deal with congestion and QoS), WiFi networks' ability to guarantee QoS depends not only on coverage but also on the traffic load generated by those stations sharing the channel. Therefore, despite available QoS mechanisms [12], a congested WiFi network may be unable to meet the strict QoS requirements of interactive real-time services such as VoIP [13–16]. Unfortunately, this fact is typically ignored in studies of UAV-AP link performance [17,18].

It is proven that there is an upper bound in the number of VoIP traffic flows that an AP can handle with acceptable performance, namely VoIP capacity [19]. As the authors in [13] put it, above this upper bound, "*One more VoIP connection will jeopardize the performance of all voice connections*". The VoIP capacity of an AP can be studied through a model of the Medium Access Control (MAC) sub-layer [19] which lets us estimate the impact of VoIP traffic in delay or packet loss [20,21]. Applying the findings from this research field to the problem of UAVs optimal positioning would allow one to consider the maximum number of simultaneous calls that each UAV-mounted AP can take (i.e. VoIP capacity) to guarantee QoS requirements. Furthermore, VoIP capacity should also consider statistical multiplexing in the service demand since it is unlikely that all users associated to an AP use the VoIP service concurrently. However, all this has been overlooked in existing UAVs optimal location problems [22,23]

In this work, we define and solve a new optimization problem that consists of finding the minimum number of UAV-mounted APs that should be launched to provide VoIP service with guaranteed QoS and

* Correspondence to: C/Camino de los descubrimiento s/n., 41092, Seville, Spain.
E-mail addresses: vmayor@trajano.us.es (V. Mayor), rafa@trajano.us.es (R. Estepa), aestepa@trajano.us.es (A. Estepa), german@trajano.us.es (G. Madinabeitia).

https://doi.org/10.1016/j.comcom.2022.06.037
Received 4 March 2019; Received in revised form 16 July 2019; Accepted 22 June 2022
Available online 28 June 2022

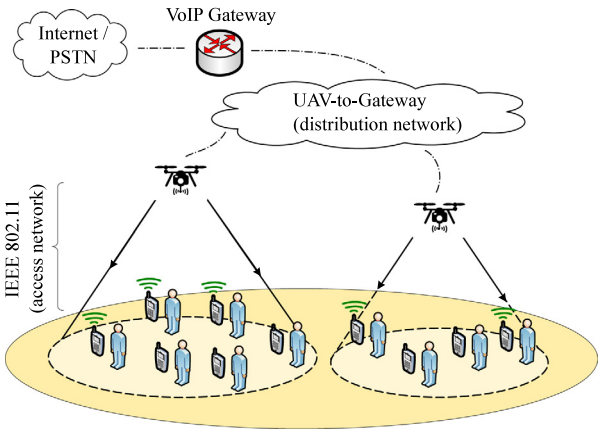

Fig. 1. Example scenario for VoWiFi.

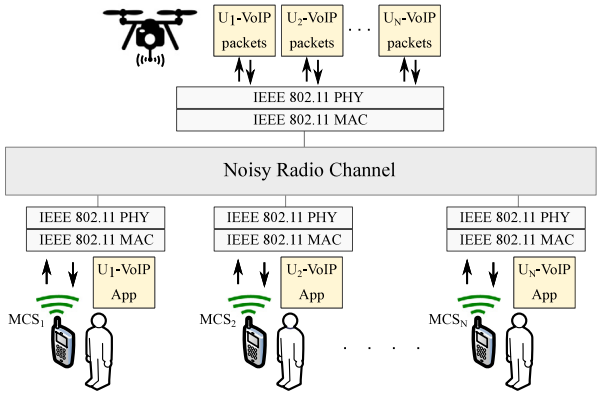

Fig. 2. UAV-AP: IEEE 802.11 system under consideration.

call-blocking probability to a set of known users in a scenario that lacks alternative cellular or WiFi infrastructure on ground (see Fig. 1[1]). More specifically, our problem provides the minimum number of UAVs to be deployed and their optimal location so that VoIP capacity of any deployed AP is equal to or greater than the number of users associated to that AP who are expected to be simultaneously talking.

Most handheld devices (e.g. smartphones, tables) have WiFi. Thus, a VoWiFi service can be of potential interest in situations where users are expected to be confined in known areas such as meeting points during search and rescue missions, for broadcast announcements, or voice service during outdoor activities or missions in remote areas that lack alternative communication infrastructure. Indeed, in these contexts, a common VoIP application could be downloaded by users from the UAV-deployed WiFi data access network. We also provide a preliminary analysis of the applicability of our problem where user mobility is considered.

The contributions and originality of this paper are:

- We mathematically formulate a new optimal drone location problem that considers the speech quality perceived by ground users and the call-blocking probability.
- We provide a mathematical model to predict speech quality for a set of heterogeneous VoIP traffic sources and different IEEE 802.11 standard amendments.
- We propose a service model that takes advantage of statistical multiplexing of users' calls, providing efficient use of resources.

2. QoS in VoIP over WiFi networks

ITU-R rec. M.1079 indicates that each communication service requires specific ranges of end-to-end delay, loss and jitter to be met, and VoIP is no exception. In our view, planning a VoIP service over IEEE 802.11 networks requires taking into account two key aspects:

1. The speech quality of the VoIP service, defined by the ITU-T rec. P.800 [24], which is measured through surveys that rate a mean opinion score (MOS) ranging from 1 (poor) to 5 (excellent).
2. The probability that a user cannot place a new call as a result of the exhaustion of the resources of the (WiFi) network. This is also known as call-blocking probability in the field of teletraffic.

[1] Observe that the performance of the WiFi access network (see Fig. 1) is assumed to be critical for the feasibility of the QoS-guaranteed service. At the same time, we assume that UAV-to-UAV, or UAV-to-Infrastructure either do not significantly impair the QoS, or its impact can be added to our model as a constant extra delay and/or loss. Therefore, the scope of this paper is restricted to the IEEE 802.11 access network to be deployed.

Table 1
802.11 sensitivity relations for OFDM modulations with 20 MHz channels.

Modulation	Coding rate	Data rate (Mb/s)	Sensitivity (dBm)
BPSK	1/2	6	−82
BPSK	3/4	9	−81
QPSK	1/2	12	−79
QPSK	3/4	18	−77
16-QAM	1/2	24	−74
16-QAM	3/4	36	−70
64-QAM	2/3	48	−66
64-QAM	3/4	54	−65

According to ITU-T G.107, acceptable conversations should exhibit MOS > 3.5, but in general, if the network fails to underpin a minimum level MOS_{min}, the service simply cannot be provided [25].

At the planning stage, a method for MOS prediction is needed. In VoIP, the most extended method is the E-Model, [26,27], which combines additive impairments factors to measure speech quality R factor, ranging from 0 (poor) to 100 (excellent), that can be directly mapped to MOS [28]. As *Assem et al.* [29] put it, the E-Model is "a repeatable way to assess if a network is prepared to carry a VoIP call or not". In its simplest form, the E-model can be expressed as [30]:

$$R = 94.2 - I_d - I_{e-eff} \quad (1)$$

where I_d represents all impairments due to delay, and I_{e-eff} is a factor that accounts for the impairments caused by low bit-rate coding and packet loss [31]. Both, delay and packet loss are affected by the performance of the IEEE 802.11 access network.

Fig. 2 illustrates a set of IEEE 802.11 stations associated to one UAV-mounted AP. Each station is represented by its physical layer and its medium access control (MAC) sub-layer. All stations share a common MAC protocol and each one auto-configures its Modulation and Coding Schema (MCS) according to the Received Signal Strength Indicator (RSSI) from the AP and some thresholds (i.e. minimum input sensitivity) defined by the IEEE 802.11 standard in use [32]. Table 1 shows examples of different MCSs defined for OFDM modulations (e.g. IEEE 802.11a/g). Thus, each user terminal is assumed to auto-configure its MCS to the greatest bit-rate possible depending on the received signal power.

In VoWiFi, speech quality is strongly influenced by the delay and loss of the downlink (i.e. from the access point (AP) to VoIP terminals) [16]. Both factors depend on the traffic load, which in turn depends on the speech codec and the number and data bit-rate of users engaged on active calls at a given moment.[2] WiFi analytical models

[2] This assumes that either only VoIP traffic exists, or that VoIP traffic is prioritized using IEEE 802.11e.

let us capture the relation between the VoIP traffic volume handled by an AP and the delay and loss that such traffic will experience. There is a plethora of analytical models of the IEEE 802.11 MAC behavior [33–36]. In most models, the central variable is the probability that an observed station attempts to transmit in a random time slot (τ). However, different models apply different assumptions to derive their analytical expression for τ. In this paper, the following assumptions are considered:

- Heterogeneous traffic sources (two users may have different physical data bitrate according to their RSSI).
- Non-saturated stations (sometimes there may be no packets to be transmitted).
- Noisy channel (channel noise can corrupt packets).

But above analytical models, intuition suggests that VoIP traffic increases with every new call, which impacts network delay and loss, deteriorating the QoS of ongoing calls. As a result of the previous consideration, a VoWiFi service with guaranteed QoS should not accept a new call when this implies that calls in progress may turn unacceptable (i.e. MOS < MOS_{min}). This is known as Call Admission Control (CAC) function, typically implemented either at the AP (as indicated in IEEE 802.11e), or at the application level (e.g. VoIP gateway). Obviously, this function requires assessing the maximum number of concurrent calls that an AP can take so that the quality experienced by active users is above MOS_{min}. This upper bound is the VoIP capacity of an AP and will be denoted by CC_{max} from now on. For example, in [16] it was found that a maximum of 15 calls for 64 kb/s CBR VoIP traffic, or 38 calls for VBR VoIP traffic can be held for IEEE 802.11b.

This leads us to the second factor deemed as key for dimensioning: the call-blocking probability, or, equivalently, the probability that a new call is rejected as a result of CC_{max} calls being already in progress. It is possible to find such a probability if one takes a statistical model of the user behavior from the field of teletraffic. Assuming that call attempts and calls duration follow exponential distributions, the call-blocking probability for the users served by an AP is given by the classical Engset formula [37]:

$$B(A,\ u,\ cc) = \frac{\binom{u-1}{cc} A^{cc}}{\sum_{i=0}^{cc} \binom{u-1}{i} A^{i}} \tag{2}$$

where A stands for the traffic intensity (product of average frequency and duration of calls), u is the number of users associated to the access point, and cc is the number of concurrent calls.

Then, provisioning VoWiFi with guaranteed QoS will require that the following constraints are met:

- Speech quality level (MOS) higher than MOS_{min}.
- Call-blocking probability lower than $B_{\text{max}} = B(A, u, \text{CC}_{\text{max}})$.

which will be regarded as VoWiFi service QoS constraints in the problem to be defined next.

3. Problem statement

In the scenario illustrated in Fig. 1, we want to deploy a set of drones to create a WiFi access network that enables the VoWiFi service with guaranteed QoS. To make the problem more tractable, the following assumptions are made:

- The position of ground users is known. User terminals run a VoIP app which utilizes a known codec and standard signaling.
- If a ground terminal could associate to more than one AP, the one with maximum received power will be selected.
- Channelization between adjacent APs is done in such a manner that interferences are negligible.
- A CAC mechanism is in place to limit the maximum number of concurrent calls at each AP.

3.1. Terminology

We discretize the flying zone as illustrated in Fig. 3. The set $\mathcal{P}$ represents the set of $\mathbb{R}^3$ coordinates of each edge of the grid (i.e. potential locations of UAVs). The following terms and definitions will be used for the remainder of this paper:

- Users are denoted by the set $\mathcal{U} = \{1, 2, \dots, U\}$ and at known locations given by $\{\boldsymbol{w}_k | k \in \mathcal{U}\}$, where $\boldsymbol{w}_k \in \mathbb{R}^3$ represents the 3D coordinates of user k.
- Drones are denoted by the set $\mathcal{D} = \{1, 2, \dots, D\}$ and at known locations given by the set $\mathcal{X} = \{\boldsymbol{x}_1, \boldsymbol{x}_2, \dots, \boldsymbol{x}_D | \boldsymbol{x}_i \in \mathcal{P}, i \in \mathcal{D}, \boldsymbol{x}_i \neq \boldsymbol{x}_j|_{\forall j \neq i}\}$, where $\boldsymbol{x}_i \in \mathcal{P}$ represents the 3D coordinates of dron i.
- $C(i) \subset \mathcal{U}$ represents the set of users associated to the access point at drone $i \in \mathcal{D}$.
- The number of ground users associated to the WiFi network is $C = \sum_{i=1}^{D} |C(i)|$.
- $B(i)$ represents the call-blocking probability for users associated to the access point at drone $i \in \mathcal{D}$.
- $MOS(i)$ represents the speech quality level for users associated to the access point at drone $i \in \mathcal{D}$.

Fig. 3, illustrates a scenario with 12 users ($U = 12$) and two drones ($D = 2$). The UAVs flying space has been discretized using a grid $\mathcal{P}$ with 30 edges. The set $\mathcal{D} = \{1, 2\}$ is composed by the leftmost drone (located at $\boldsymbol{x}_1 \in \mathcal{P}$) and the rightmost drone (at $\boldsymbol{x}_2 \in \mathcal{P}$). Then, $C(1)$ and $C(2)$ would be composed of the set of users associated to drones 1 and 2 respectively, and the ratio of users associated to the WiFi network would be $\sum_{i=1}^{2} |C(i)|/U = 11/12$.

3.2. Problem definition

Our goal is to minimize the number of drones deployed. Among solutions with the same number of drones, we chose the one that minimizes the ratio of uncovered users (i.e. terminals not associated to the WiFi network). This can be formulated as follows:

$$\begin{aligned} \min_{\mathcal{X}} \quad & D + \left(1 - \sum_{i=1}^{D} |C(i)|/U\right) \\ \text{subject to} \quad & \sum_{i=1}^{D} |C(i)|/U \geq C_{\text{min}} \\ & B(i) \leq B_{\text{max}} \quad , \forall i \in \mathcal{D} \\ & MOS(i) \geq \text{MOS}_{\text{min}} \quad , \forall i \in \mathcal{D} \\ & \boldsymbol{x}_i \in \mathcal{P} \quad , \forall i \in \mathcal{D} \\ & D \leq D_{\text{max}} \end{aligned} \tag{3}$$

where D represents the cardinality of $\mathcal{D}$ (which is bounded by D_{max}), and $(1 - \sum_{i=1}^{D} |C(i)|/U)$ is the ratio of ground users uncovered. Constants C_{min}, B_{max}, MOS_{min} are thresholds for their respective constraints. According to ITU-T G.107 recommendation, an acceptable call should exhibit a $MOS >\sim 3.5$. But one could decide to raise that lower bound to provide a higher quality service. This would impact on the number of drones deployed (e.g. more UAVs may be necessary to provide the voice service as the VoIP capacity of APs is decreased).

Finally, observe that the objective function is composed of an integer (i.e. number of UAVs, $D \geq 1$), and a decimal number (the ratio of uncovered users < 1). Thus, the integer part indicates the minimum number of UAVs that meet all constraints.

4. Finding solutions using exhaustive search

The exhaustive search approach involves assessing (3) all possible UAV(s) positions within the grid ($\mathcal{P}$) for an incremental number of drones until the optimal solution is found (or a maximum number of

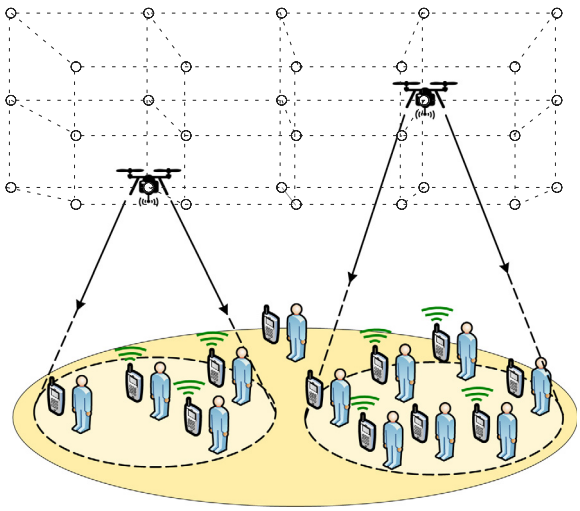

Fig. 3. Grid edges in a deployment scenario.

UAVs $D_{\max}$ is reached). This procedure is described in Algorithm 1. It takes as input the set of ground users $\mathcal{U}$ and their location, the set of edges $\mathcal{P}$, $D_{\max}$, and the coverage and QoS constraints. All possible combinations of UAVs locations are checked for an incremental number of drones (D). The algorithm starts by estimating the set of users associated to the WiFi network formed by D drones located at $\mathcal{X}$. If the first constraint (i.e. coverage) is met, then QoS constraints are assessed (considering the worst case among all UAVs). If both constraints are met, a potential solution is found, and the objective function is evaluated. Among the potential solutions with the same value of D, the one with the lowest objective function is selected. The algorithm ends after finding the optimal solution or trying unsuccessfully with $D_{\max}$ drones. The algorithm's output is the set of optimal UAVs locations and the value of the objective function. A null location indicates that no solution has been found.

Input: $\mathcal{U}$, $\{\boldsymbol{w}_k\}$, $D_{\max}$, $C_{\min}$, $B_{\max}$, $MOS_{\min}$
Output: $\mathcal{L}$ (location), $of_{\min}$ (obj. function)
Initialization: $D = 1$, $\mathcal{L} = \emptyset$, $of_{\min} = D_{\max} + 1$

while $\mathcal{L} = \emptyset$ **or** $D \leq D_{\max}$ **do**
  D++; // Increase number of UAVs
  foreach *possible value of* $\mathcal{X}$ **do**
    for $j = 1$ **to** D **do**
      $C(j) = associate(\mathcal{U}, \{\boldsymbol{w}_k\}, \mathcal{X})$;
    end
    /* check first constraint */
    if $\left(\sum_{i=1}^{D} |C(i)|/U\right) \geq C_{\min}$ **then**
      for $j = 1$ **to** D **do**
        $\text{MOS}(j) = QoS.eval(C(j), \boldsymbol{x}_j, \{\boldsymbol{w}_k\}, B_{\max})$;
      end
      $\text{MOS} = \min_{k=1..D} \{\text{MOS}(k)\}$;
      if $MOS \geq MOS_{\min}$ **then**
        /* QoS constraints met */
        $of = D + (1 - \sum_{i=1}^{D} |C(i)|/U)$;
        if $of < of_{\min}$ **then**
          $of_{\min} = of$; // solution
          $\mathcal{L} = \mathcal{X}$; // UAVs position
        end
      end
    end
  end
end

Algorithm 1: Exhaustive search pseudocode

Next, we elaborate on the functions used for the assessment of signal coverage and the constraints related to quality of service.

4.1. Signal coverage evaluation: associate()

A ground terminal associates to an AP if its Signal to Noise Ratio (SNR) and Received Signal Strength Indication (RSSI) are above minimum levels to properly demodulate the received signal. In addition, if several APs were available (e.g. $D > 1$), each user will be associated to the AP with maximum received power.

The UAV-to-ground path loss should generally consider a combination of Line-of-Sight (LoS) and NLoS components whose probability depend on the drone altitude and ground terminal surroundings [38]. We adopt the model presented in [39] (also used in [4]). According to such model, the probability that a ground user has a LoS link with the AP installed at a drone is:

$$P_{LoS}(\theta) = \frac{1}{1 + a_1 e^{-b_1 \theta \cdot 180/\pi + b_1 a_1}} \tag{4}$$

where θ is the elevation angle in degrees (between user and drone), a_1 and b_1 are environment dependent constants (e.g. rural, urban, etc.). Then, for user i located at $\boldsymbol{w}_i$ and the AP installed at drone j located at $\boldsymbol{x}_j$, $RSSI_{ij}$ is given by:

$$\begin{aligned} \text{RSSI}_{ij} =& P_{TX} + G_{ij} - 20 \log_{10}\left(\frac{4\pi f \cdot \|\boldsymbol{w}_i - \boldsymbol{x}_j\|}{c}\right) \\ & - P_{LoS}(\theta_{ij}) \cdot \eta_{LoS} - (1 - P_{LoS}(\theta_{ij})) \cdot \eta_{NLoS} \end{aligned} \tag{5}$$

$$G_{ij} = 10 \ \log_{10}(10^{G_{\max}/20} \cdot \cos^2 \theta_{ij}) \tag{6}$$

where P_{TX} (dBm) stands for the power delivered by the transmitter antennas; G_{ij} stands for the gain of the antenna between user i and UAV j as indicated in (6); $\|\boldsymbol{w}_i - \boldsymbol{x}_j\|$ is the Euclidean distance between user i and drone j; f (hertz) is the channel frequency; c (m/s) is the speed of light; θ_{ij} (radians) accounts for the elevation angle between user's position $\boldsymbol{w}_i$ and UAV's position $\boldsymbol{x}_j$; η_{LoS} (in dB) and η_{NLoS} (in dB) are losses corresponding to LoS and NLoS connections which depend on the environment (a list of values can be found in [40]). Finally, constant $G_{\max}$ in (6) indicates the maximum power.

Given RSSI_{ij}, the *Signal to Noise Ratio* (SNR_{ij}) (dB) can be readily obtained by subtracting the receiver's noise figure (NF) and thermal noise (N) as indicated in (7) and (8).

$$\text{SNR}_{ij} = \text{RSSI}_{ij} - NF - N \tag{7}$$

$$N = -174 + 10 \ \log_{10}(C_{BW}) \tag{8}$$

where C_{BW} stands for signal bandwidth as specified by the IEEE 802.11 standard in use.

For all $i \in \mathcal{U}$ and for all $j \in \mathcal{D}$, let us define γ_{ij} as a boolean variable that indicates whether user i satisfies minimum thresholds (i.e. $\text{SNR}_{ij} \geq \text{SNR}_{\min}$ and $\text{RSSI}_{ij} \geq \text{RSSI}_{\min}$) with respect to UAV j or not. Then, the function *associate()* returns the set of users that meet minimum thresholds and whose RSSI with drone j is greater than with any other drone:

$$C(j) = \{i \in \mathcal{U} \mid \gamma_{ik} = 1, \ \text{RSSI}_{ij} > \text{RSSI}_{ik} \ \forall k \neq j\} \tag{9}$$

Recall from previous section that each ground user's terminal i sets its *Modulation and Coding Scheme* $\text{MCS}^{(i)}$ according to its $\text{RSSI}^{(i)} = \max_{j=1..D}\{\text{RSSI}_{ij}\}$ (see (5)), which determines the data bit rate of the terminal.

4.2. VoWiFi service QoS evaluation: QoS.eval()

This function checks on VoWiFi service QoS constraints described in Section 2 by following these two broad steps:

Input: $|C(j)|$ (set of users associated), A, $B_{\max}$
Output: $CC_{\max}$ (maximum concurrent calls)

```
for cc = 1 to |C(j)| do
    if B(A, |C(j)|, cc) ≤ B_max then        // Eq. (2)
        CC_max = cc;
        cc++;
    end
end
```

Algorithm 2: Finding $CC_{\max}$ within an AP

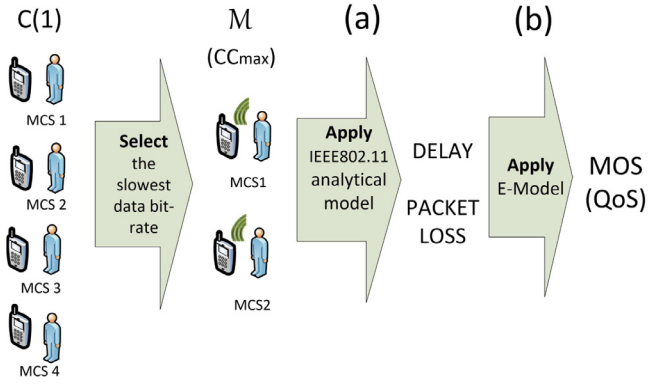

Fig. 4. For QoS assessment.

1. Find out how many users in $C(j)$ can simultaneously talk so that the call-blocking probability $B_{\max}$ is not exceeded (i.e. find $CC_{\max}$). This can be readily done by increasing the number of concurrent calls in (2) as indicated in Algorithm 2.
2. Estimate the MOS: Let $\mathcal{M} \subset C(j)$ be the subset composed of the CC_{max} stations with the lowest data bit rate in $C(j)$. Stations in $\mathcal{M}$ are expected to exhibit greater transmission/reception delay than the rest and consequently, are regarded to be "worst case" in terms of QoS. First, an analytical model of the IEEE 802.11 mac sub-layer is applied to the system composed of the set of stations $\mathcal{M}$ plus its AP to estimate the delay and packet loss experienced by VoIP traffic. Then, the E-model is used to finally obtain speech quality level MOS. This is illustrated in Fig. 4. Next we elaborate on steps (a) and (b).

Delay and packet loss estimation. The set of stations in $\mathcal{M}$ and its AP constitute a IEEE 802.11 system whose performance has been largely studied in scientific literature [41–44]. We have used a mix of different analytical models from [33–36] fitted for the following assumptions: stations can have different bit rates (i.e. heterogeneous traffic sources), stations are not-saturated,[3] and the channel is noisy. Due to the complexity of the subject, and for the sake of clarity, we keep this section as simple as possible. The reader is encouraged to read more elaborated information in the corresponding references and Appendix A.

The *Distributed Coordination Function* (DCF) of the 802.11 MAC sub-layer use CSMA/CA (*Carrier Sense Multiple Access with Collision Avoidance*) for medium access control. Basically, each contending station must sense the medium during a period of time in order to ensure that it is idle before transmission. If the channel is busy, the station waits a random backoff interval before trying again. The backoff process is based on the *Binary Exponential* algorithm. Time is discretized and the algorithm picks a random number of time slots between 0 and $2^i W_o$, where W_o accounts for the minimum contention window value, and i increases by one in each failed attempt up to a ceiling m. After a maximum number of retransmissions is reached (M), the packet is discarded.

Most analytical models based on Markov chains lay on a central variable termed τ which represents the probability that an observed station attempts to transmit in a randomly chosen time slot. In this paper we used the expression in [33]:

$$\tau = \frac{1}{\eta}\frac{1}{1-q}\left(\frac{r^2 W_o}{(1-p)(1-(1-r)^{W_o}} - qr(1-p)\right) \tag{10}$$

where η is defined in (14), q is the probability of having at least one packet queued at the transmission buffer, p is the probability that a packet suffers any transmission errors, and r is the probability that at least one packet arrives during an idle state (load factor). Assuming non-saturated stations and Poisson packet arrivals (with rate λ) to the transmission queue, r and q can be expressed as:

$$r = 1 - e^{-\lambda E[T]} \tag{11}$$

$$q = 1 - e^{-\lambda E[T] E[B]} \tag{12}$$

where $E[T]$ represents the expected average slot duration, and $E[B]$ is expected average number of back-off slots that a packet waits before transmission. Due to its complexity, a closed-form of $E[T]$ is deduced in Appendix A (Eq. (A.19)). $E[B]$ can however, be expressed as in [36]:

$$E[B] = \frac{W_o}{2(1-p)}\left(\frac{1-p-(2p)^m}{(1-2p)} - 2^m p^{M+1}\right) \tag{13}$$

$$\begin{aligned}\eta = {} & (1-r) + \frac{r^2 W_o (W_o+1)}{2(1-(1-r)^{W_o})} \\ & + \frac{W_o+1}{2(1-q)}\left(\frac{r^2 q W_o}{1-(1-r)^{W_o}} + rp(1-q) - rq(1-p)^2\right) \\ & + \frac{p}{2(1-q)(1-p)}\left(\frac{r^2 W_o}{1-(1-r)^{W_o}} + qr(1-p)^2\right) \\ & \times \left(2W_o \frac{1-p-p(2p)^{m-1}}{1-2p} + 1\right)\end{aligned} \tag{14}$$

Let $\tau^{(i)}$, $r^{(i)}$, $q^{(i)}$, $E[B^{(i)}]$ and $\lambda^{(i)}$ denote τ, r, q, $E[B]$ and λ of station i in the system under consideration (i.e. the subset $\mathcal{M}$ and its AP such as illustrated in Fig. 2), where i refers to either one user station $\{1, 2, ..|\mathcal{M}|\}$, or the AP ($i = |\mathcal{M}| + 1 = AP$). Let $p^{(i)}$ be the probability of packet transmission error p for station i. Then, $p^{(i)}$ can be broken down as:

$$\begin{aligned} p^{(i)} &= \left(1 - P_i^{(i)}\right) \cup \mathrm{FER}^{(i)} \\ &= \left(1 - P_i^{(i)}\right) + \mathrm{FER}^{(i)} - \left(1 - P_i^{(i)}\right) \cdot \mathrm{FER}^{(i)} \end{aligned} \tag{15}$$

where $P_i^{(i)}$ accounts for the probability that the jth station finds the channel idle and $\mathrm{FER}^{(i)}$ stands for the Frame Error Rate due to channel noise. The probability of finding the channel idle, can be further expressed as:

$$P_i^{(i)} = \prod_{j=1,\ i\neq j}^{S} \left(1 - \tau^{(j)}\right) \tag{16}$$

Assuming that frames have a constant size of L bits (L = preamble + header + data), it is possible to obtain the FER of station i as:

$$\mathrm{FER}^{(i)} = 1 - (1 - \mathrm{P}_e^{(i)})^L \tag{17}$$

where $\mathrm{P}_e^{(i)}$ represents the codec bit error rate of station i, which can be readily calculated[4] if one knows user's modulation (i.e. $\mathrm{MCS}^{(i)}$).

Finally, solving the non-linear equation system, the *packet loss* of station i can be expressed as:

$$\mathrm{PL}^{(i)} = 1 - \frac{\left(1 - \mathrm{FER}^{(i)}\right)\tau^{(i)} \prod_{j=1, j\neq i}^{|\mathcal{M}|+1}\left(1-\tau^{(j)}\right)}{\lambda^{(i)}\ E[T]} \tag{18}$$

[3] When the channel is idle a station may have no packets to transmit.

[4] See equations in [45] and [46] for DSS and OFDM modulations respectively.

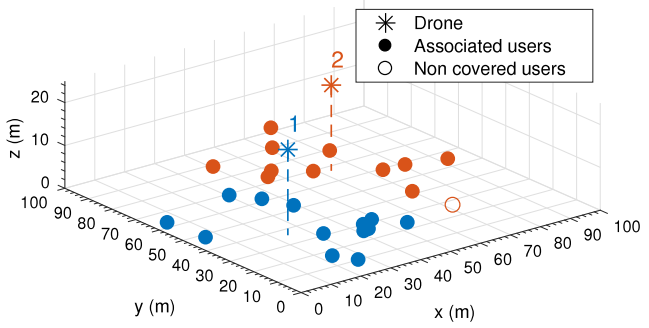

Fig. 5. Example solution ($D = 2$).

Since we assume a very small buffer size, the queueing delay can be neglected, and the only delay component will be the channel access delay. Then, the delay of station i can be expressed as:

$$\mathrm{DEL}^{(i)} = E[B^{(i)}]\ E[T] \tag{19}$$

As justified in [16], the AP[5] ($i = AP$) is the most saturated station, leading the packet loss and delay in the system. Thus, we can take its packet loss and delay as representative of the worst case. Then, the output of this step is:

$$\mathrm{PL} = \mathrm{PL}^{(AP)} \tag{20}$$

$$\mathrm{DEL} = \mathrm{DEL}^{(AP)} \tag{21}$$

MOS estimation. As stated in Section 2, the E-Model rates the conversation quality R factor, which can be calculated using (1) [29], whose terms were:

- $I_{e,eff}$ is the effective impairment equipment parameter. It is a combination between impairment equipment parameter at zero packet loss (I_e), and a function of I_e that is dependent on packet loss rate and packet loss behavior. It can be expressed as:

$$I_{e,eff} = I_e + (95 - I_e)\frac{P_{pl}}{\frac{P_{pl}}{\mathrm{BurstR}} + B_{pl}} \tag{22}$$

  where I_e is a codec-dependent constant associated with codec compression degradation,[6] P_{pl} represents the packet loss rate, BurstR accounts for the burst ratio (i.e. equals 1 if packet loss if random and greater otherwise), B_{pl} represents the codec packet loss robustness, which also has a specific value for each codec (listed in ITU-T Rec. G117 Appendix I).
- I_d accounts for all impairments due to delay of communication chain. A widely accepted approximation for I_d can be obtained from one-way delay in communication path (d) as follows:

$$I_d = 0.024d + 0.11(d - 177.3)H(d - 177.3), \tag{23}$$

  where H is the Heaviside function (i.e. $H(x) = 0$ for $x < 0$ and $H(x) = 1$ for $x > 0$). This shows that the effect of one-way delays under 100 ms can be discarded.

In this paper, we will use the G.711 codec ($I_e = 0$) with BurstR = 1 and $B_{pl} = 25,1$. So, assuming that $P_{pl} = \mathrm{PL}$ (from (20)), and $d = \mathrm{DEL}$ (from (21)) + 20 ms (from the VoIP codec packetization), R can be expressed[7] as:

$$R = 93.72 - 95\frac{\mathrm{PL}}{\mathrm{PL} + 25,1} - (0.024\mathrm{DEL} + 0.11(\mathrm{DEL} - 157.3)H(\mathrm{DEL} - 157.3)) \tag{24}$$

Finally, to obtain speech quality, the R factor can be mapped to MOS [27] as:

$$\mathrm{MOS} = \begin{cases} 1, & R < 6.5 \\ 1 + 0.035\ R + 7 \cdot 10^{-6}\ R \\ \quad \cdot (R - 60)\ (100 - R), & 6.5 \le R \le 100 \\ 4.5, & R > 100 \end{cases} \tag{25}$$

4.3. Example solution

In this section, we provide an example solution obtained after implementing Algorithm 1 in Matlab® in a scenario that includes 25 ground users randomly distributed within an area of 100 m×100 m. The parameters used are listed in Table 3. Unless otherwise specified, such parameters are common to all experiments in this paper.

Fig. 5 ilustrates the solution obtained. Users' color shows the user distribution among UAVs. In this case, two drones were required to cover 24 out of 25 users[8] (i.e. $(|\mathcal{C}(1)| + |\mathcal{C}(2)|)/U = 0.96 > C_{\min}$) using the IEEE 802.11n standard revision.

The solution represented in Fig. 5 has been simulated with the network simulator ns-3 in order to validate the IEEE 802.11 analytical model from Section 4.2. The ns-3 model *YansWifiPhy* has been used with a transmission buffer size of one packet. The simulation has been repeated 30 times with different seeds and the results presented represent the average value with a 95% confidence interval.

In Table 2, we compare the delay, packet loss and MOS from our analytical models with those obtained with *ns-3*. It can be observed no significant differences between the output of the analytical models used and simulation results, particularly in terms of predicted speech QoS. Note that delay is very small in absolute terms, always under 1 ms as a result of a very small buffer. The comparison of the MOS obtained with our analytical models versus simulation suggests that the method and models proposed in Section 4.2 are acceptable.

Note that the X–Y discretization step in our example was only 1 m (which we consider the minimum safe for collision avoidance), while Z step was 5 m. In general, the smaller grid steps the more accurate the solution will be (i.e. closer to the optimal that would be found without discretizing the flying space) but the more edges in $\mathcal{P}$ will have to be assessed, increasing the computational load. In general, $\sum_{d=1}^{D}\binom{|\mathcal{P}|}{d}$ possibilities will have to be assessed when D drones are being evaluated. For example, the grid defined in our example has $|\mathcal{P}| = 2 \cdot 10^4$ edges, thus $\simeq 2 \cdot 10^8$ possible combinations of UAV locations have been assessed. This fact suggests that exhaustive search may be feasible only in very small scenarios since its computational complexity grows exponentially with D. For that reason, heuristic search methods are commonly preferred as a general way to find (semi) optimal solutions.

5. Heuristic solution

A number of different metaheuristics can be used to find (semi)optimal solutions. These include genetic algorithms (GAs), particle swarms optimization, artificial immune system, and simulated annealing. Furthermore, other approaches such as optimal transport theory have been also successfully applied to solve user–drone association in similar scenarios.

Our heuristic search method can be viewed as a replacement of lines 3–20 in Algorithm 1 with a function call (*GAsearch*) that returns

[5] Observe that the AP is also part of the system and its MCS and FER change dynamically according to its communication partner. Our approach is to consider average values of its data bit-rate and FER.

[6] A list of values from ITU-T codecs were presented in ITUT-T Rec. G.113 Appendix I.

Table 2
Comparison of algorithmic results with simulation.

Drone (i)	x_i	$C(i)$	$B(i)$ (%)	Algorithm 1/Simulation PL (%)	D (ms)	MOS [1–4.5]
1	(24, 36, 20)	12	1.58	0.45/0.32 ± 0.05	0.19/0.12 ± 0.002	4.39/4.40
2	(63, 67, 20)	12	1.58	0.36/0.26 ± 0.04	0.18/0.13 ± 0.002	4.39/4.40

Table 3
Example solution input parameters.

IEEE Standard		Scenario		Traffic		Constraints	
Revision	802.11 n	Users	25	Calls/hour/user	1	$RSSI_{min}$	−82 dBm
GI	800 ns	Size	100 × 100 m	Call length	180 s	SNR_{min}	20 dB
Preamble	Greenfield	X–Y step	1 m	VoIP codec	G.711	MOS_{min}	3.5
Bandwidth	20 MHz	Altitude layers	{20, 25} m	On/Off times	CBR	C_{min}	0.9
Retries	7	Prop. Exponent	3.3	Packet interval	20 ms	B_{max}	0.05

Input: $\mathcal{U}$, $\{\boldsymbol{w}_k\}$, $D_{\max}$, $C_{\min}$, $B_{\max}$, $MOS_{\min}$
Output: $\mathcal{L}$ (location), $of_{\min}$ (obj. function)
Initialization: $D = 0$, $\mathcal{L} = \emptyset$, $of_{\min} = D_{\max} + 1$
1 **while** ($\mathcal{L} = \emptyset$ ***or*** $D \leq D_{max}$) **do**
2 $\quad D++$;
3 $\quad \mathcal{L}, of$ = *GAsearch*(D, $\{\boldsymbol{w}_k\}$, $B_{\max}$, $C_{\min}$, $\text{MOS}_{\min}$)
4 **end**

Algorithm 3: Use of the heuristic search method

the (semi)optimal solution found for a specific number of drones D as shown in Algorithm 3.

We have designed the genetic algorithm *GAsearch()* using the Matlab® R2017 A Global Optimization Toolbox [47]. Next we elaborate on the GA developed.

5.1. Individuals

An individual is a possible solution to the problem. As such, each individual is a location of D drones $\mathcal{X} = \{\boldsymbol{x}_1, \boldsymbol{x}_2, \ldots, \boldsymbol{x}_D | \boldsymbol{x}_i \in \mathcal{P}, i \in D, \boldsymbol{x}_i \neq \boldsymbol{x}_j|_{\forall j \neq i}\}$, where $\boldsymbol{x}_i \in \mathcal{P}$ represents the 3D coordinates of drone i. For instance, an individual composed of two drones $\{\boldsymbol{x}_1, \boldsymbol{x}_2\}$ is given by the sequence of genes $\{x_1, y_1, z_1, x_2, y_2, z_2\}$.

5.2. Algorithm steps

The algorithm performs the following steps:

1. Generate the **initial population**.
2. Each individual from the generation is **evaluated** and ranked by assessing a *raw fitness score* based on the objective function of the problem (3).
3. **Selection** of parents according to their position in the ranking.
4. A new generation is created as follows:
   - The top 5% of the ranking (elite individuals) are copied to the new generation.
   - Of the remaining individuals:
     - 80% is created by **Crossover-and-Mutation** (CM) combining the genes of two selected parents (crossover) and applying a mutation to these new individuals with a very low probability p_m^{CM}.
     - 20% is created by mutation of parents (termed self-reproduction and mutation, SRM) with probability p_m^{SRM}.
5. After each new generation the **exit criteria** is evaluated. The algorithm finishes when the lowest raw fitness score found cannot be improved after MAX_G consecutive generations[9] by at least 10^{-3}. If the exit criteria is not met, go to step 2.

The previous steps differ slightly from the traditional sequential application of operations done by the canonical GA, however convergence is improved according to [48,49].

5.2.1. Initial population

It is desirable to count with initial individuals prone to be fit [50]. We created the following heuristic based on the *k-means* clusterization method illustrated in Fig. 6:

- In an area similar to the grid X–Y dimensions, D clusters are created so that the mean distance from each ground user to its cluster centroid is minimized. Then, we add the grid's average altitude to the centroid of each 2D region created previously, obtaining 3D centroids.
- The first individual of the initial population will locate its drones in the edges closest to these 3D centroids.
- The remainder $(p - 1)$ individuals of the initial population are created simply by distributing each individual's drones randomly among the spatial regions created around each centroid. In particular, we define cubes with a volume equals to the D-th part of the grid volume.[10] Note that drones are always located at grid edges

We found experimentally that a population size p of 200 individuals provided results that could not be improved in the scenarios tested.

To guarantee convergence, after creating the initial population, these 3D spatial regions are no longer taken into consideration for next generations. This implies that genes carried by individuals from next generations are not constrained by spatial regions and hence, could be at any edge $\in \mathcal{P}$.

[7] The 20 ms of packetization delay has been taken into account in the expression provided.

[8] Some ground terminals almost entirely overlap in the figure as they were generated randomly.

[9] However, if within the first MAX_G generations no individual meets problem constraints, the algorithm returns $\mathcal{L} = \emptyset$ to indicate that no solutions can be found with that number of drones.

[10] Observe that since the centroid of each cube was determined by k-means clusterization, there could be overlapping regions or regions out of the grid bounds such as those illustrated (in 2D) in Fig. 6.

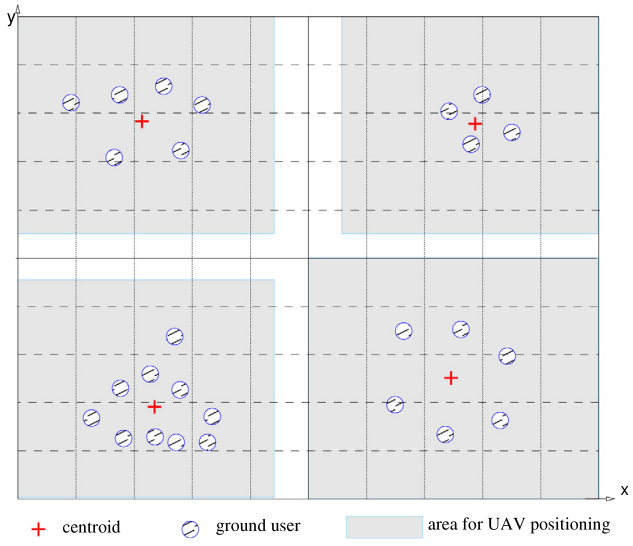

Fig. 6. Example of 2D spatial regions where drones of initial population are confined ($D = 4$).

5.2.2. Operators

The following operators have been used:

1. **Evaluation** and ranking. Each individual is assigned a raw fitness score by evaluating the problem objective function defined in (3). Since the genetic algorithm is called to search for solutions with D drones, individuals that do not meet the problem constraints are assigned a higher score by adding a penalty (between 1 and 2, according to the ratio of ground users that meet QoS constraints) to the value of their objective function. Appendix B details how the raw fitness score is calculated.
   Individuals are then sorted according to their raw fitness score. Finally, if an individual is in the n position in the ranking, it is assigned a new scored termed expectation value of $1/\sqrt{n}$.
2. Parents **Selection.** We use stochastic uniform selection among individuals according to their expectation value. In our case, 342 parents (152 × 2 CM + 38 SRM) are selected for crossover and/or mutation operations. Therefore, individuals in the top positions are chosen multiple times to be parents.
3. **Crossover.** The crossover operator combines the characteristics of two parents to create a new individual. We use a uniform crossover operation by generating a random binary vector that determines whether each child's gene comes from one parent or the other.
4. **Mutation.** We apply a exchange-type uniform mutation that consists of changing one gene of an individual with a given probability[11] (p_m^{CM} for those individuals generated after crossover, or p_m^{SRM} for parents) for a random coordinate within the grid edges.

5.3. Heuristics performance

We have carried out a series of experiments using the parameters listed in Table 4 to validate our heuristic method. In an area of 50 m × 50 m, we increase the number of users on ground from 10 to 60 so that the number of drones in the solutions is also increased. We have performed 30 runs of each experiment (changing the layout of ground user randomly each time) and thus, values shown represent the average value obtained

[11] We set $p_m^{SRM} = 1/(3 \cdot D)$ in inverse proportion to the number of genes of individuals, and $p_m^{CM} = 1/2 \cdot p_m^{SRM}$.

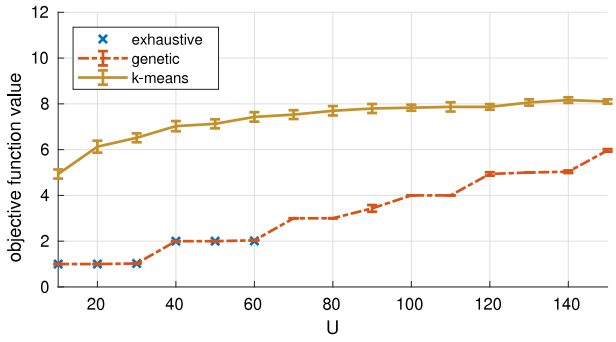

Fig. 7. Comparing heuristics, exhaustive search and clusterization.

5.3.1. Quality of the solutions

Table 5 compares the results obtained with our heuristic method, the exhaustive search method, and the results obtained by simply using the first individual in our initial population (i.e. k-means clusterization method). For each case, we show the number of drones D, the number of ground users associated to the WiFi network C, and the value of the objective function from (3). When greater than zero, the standard deviation is included between parentheses. It can be observed that results obtained with our heuristic method are very close to the optimal found by exhaustive search, matching the number of required drones in all cases. Solutions found by k-means clusterization, however, overestimate the number of drones needed, providing poor results when compared to our heuristics.

Results have been extended from 70 to 150 ground users for our heuristic method and k-means (such extension poses a computational burden too high for exhaustive search with the grid under consideration, e.g. for $D = 3$ and $|\mathcal{P}| = 2500$ edges, more than $15 \cdot 10^9$ possible UAV location combinations would have to be evaluated). Fig. 7 plots the value of the objective function in our extended comparison. Results suggest that the number of drones obtained with our heuristics tends to grow linearly with the number of users in the scenario under consideration,[12] outperforming the solutions found with k-means in the studied cases. Note that since the coverage constraint $C_{\min}$ is 0.9, the value of the objective function is almost entirely determined by the number of drones (which explains the steps in the plot). The value of the objective function exhibits greater confidence intervals in $U = 90$ as a result of finding solutions with a different number of drones (3 or 4) along with the 30 repetitions, as the user layout is randomly generated.

5.3.2. Convergence speed and complexity

Fig. 8 shows the number of generations produced by our heuristic search until a solution is found. Remember that D is increased (and a new call to GAsearch is made) only after failing to find an individual that meets the problem constraints for MAX_G consecutive generations.[13] Results show that the best individual is always found within the first five generations in all scenarios tested. This explains that solutions with D drones (see Figs. 7 and 8) are commonly found after $\sim 50D$ generations (see our exit criteria).

The fast convergence speed attained can be attributed to:

- The first generation created exhibits excellent fitness. Both the k-means clusterization heuristic, and the large population size ($p = 200$) makes a first generation of 200 individuals prone to be good candidates.

[12] The grid dimensions determine the density of ground users. Thus, for a given area of sufficient dimensions (2500 m^2 in our scenarios), the number of drones grows linearly with the density of users as shown in Fig. 7.

[13] MAX_G was determined experimentally. We initially tried $MAX_G = 200$ generations in an scenario of 100 m × 100 m and X–Y steps of 1 m. But since solutions were always found in the first five generations, we decided to set $MAX_G = 50$.

Table 4
Heuristics validation input parameters.

IEEE Standard		Scenario		Traffic		Constraints	
Revision	802.11 n	Users	$\{10, \ldots, 60\}$	Calls/hour/user	1	$RSSI_{min}$	−82 dBm
GI	800 ns	Size	50 × 50 m	Call length	180 s	SNR_{min}	20 dB
Preamble	Greenfield	X–Y step	1 m	VoIP codec	G.711	MOS_{min}	3.5
Bandwidth	20 MHz	Altitude layers	20 m	On/Off times	CBR	C_{min}	0.9
Retries	7	Prop. Exponent	3.3	Packet interval	20 ms	B_{max}	0.05

Table 5
Comparison of exhaustive, heuristic, and k-means.

U		10	20	30	40	50	60
Exhaustive	D	1	1	1	2	2	2
	C	10	20	29.27 (0.45)	40	50	59.33 (0.52)
	of	1	1	1.024 (0.02)	2	2	2.01 (0.01)
Genetic	D	1	1	1	2	2	2
	C	10	20	29.23 (0.43)	40	50	57.87 (0.35)
	of	1	1	1.026 (0.01)	2	2	2.035 (0.01)
k-means	D	4.93 (0.64)	6.1 (0.84)	6.47 (0.63)	6.97 (0.72)	7.07 (0.64)	7.37 (0.67)
	C	10	19.43 (0.5)	28.5 (0.51)	37.63 (0.72)	46.93 (0.87)	56.27 (1.17)
	of	4.93 (0.64)	6.13 (0.84)	6.52 (0.63)	7.03 (0.72)	7.13 (0.64)	7.43 (0.67)

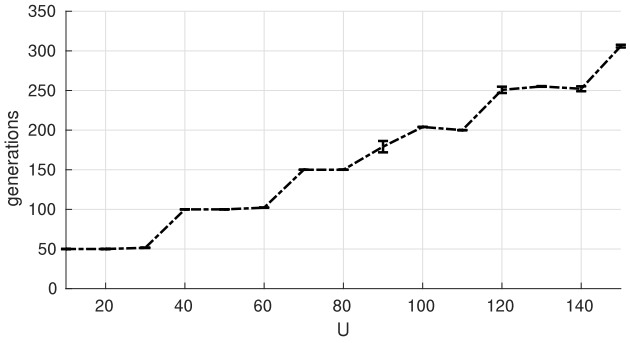

Fig. 8. Generations evaluated until exit criteria is met.

- The characteristics of the scenarios tested. Considering the finest-grained discretization X–Y step of 1 m, the number of grid edges that belong to each cluster (i.e. $|\mathcal{P}|/D$) is not too large compared to the population size used. In general, this two factors will determine the convergence speed, and thus, for scenarios covering a wider area (i.e. large $|\mathcal{P}|$) a larger population is advised to attain fast convergence.

The pseudocode used to evaluate the raw fitness function for D drones (see Appendix B) can be computed in $O(U \cdot D)$ time.[14] According to our previous convergence analysis, the fitness function is evaluated a number of times that depends on the number of generations created and population size as $\sim D \cdot MAX_G \cdot p$ (e.g.$\sim$ 10 000 $\cdot D$ in our scenario). Then, we could state that the computational complexity of our heuristic method is $O(U \cdot D^2)$. However, the number of drones used is not independent of the number of ground users. In its lower bound, D is limited by U/U_0 (where U_0 is the greatest number of ground users whose traffic can be handled by a single drone). In its upper bound, however, D tends to match the number of users U (e.g. in a large extension with scattered users). Finally, using this upper bound, we conclude that the computational complexity of our heuristic method is upper bounded by $O(U^3)$. However, if one considers that D is constrained by the maximum number of UAVs in the problem (constant D_{max}), then the computational complexity would be $O(U)$. At any rate, solutions can be computed in polynomial time.

[14] The pseudocode is composed by three main loops $O(UD)+O(UD)+O(U)$.

6. Numerical results

This section provides a numerical analysis of the proposed UAV deployment method. Results are obtained through the heuristics proposed in Section 5. The focus is set on two different aspects: the impact of the IEEE 802.11 standard revision in use, and the impact of the constraints bounds in the solutions.

6.1. Influence of IEEE 802.11 standard revision

A comprehensive study of the challenges and implications of the various IEEE 802.11 amendments in long-range outdoor WiFi deployments can be found in [23]. In this section, we compare the performance of the IEEE 802.11 (b/g/a/n/ac) standard amendments shown in Table 6 and evaluate their fitness to scenarios with specific characteristics. In particular, we define two types of scenarios:

- *Coverage-limited* scenario: for a fixed number of ground users $U = 100$, the terrain size is increased from 100 m^2 to 10 000 m^2, obtaining user sparsity ranging from 1 m^2 to 100 m^2. In this scenario type, it is expected that the number of drones in the solutions is mainly determined by the need to satisfy the coverage constraint C_{min} (which depends on the physical layer) and SNR of users.
- *QoS-limited* scenario: for a fixed very small terrain size (5 m × 5 m) the number of users is increased from 25 to 100, obtaining highly dense scenarios (1–0.25 m^2/user). In this kind of scenario, it is expected that all users are covered and the number of drones in the solutions is mainly determined by the need to satisfy QoS constraints (B_{max}, MOS_{min}) (which depend on the mac-sublayer).

Table 6
IEEE 802.11 standard revisions considered.

Frequency	Channel bandwidth	Revision
2.4 GHz	22 MHz	802.11 b
	20 MHz	802.11 g
	40 MHz	802.11 n
5 GHz	20 MHz	802.11 a
	160 MHz	802.11 ac

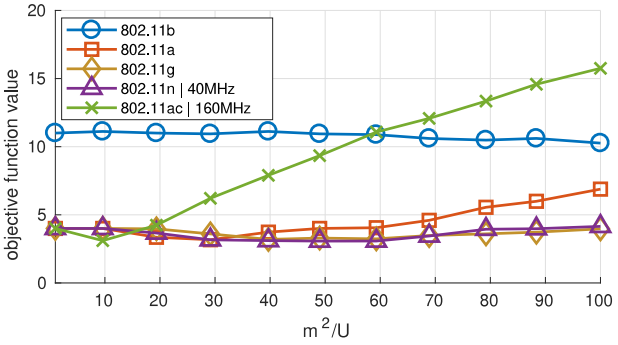

Fig. 9. Solutions for various values of user geographic dispersion.

The results presented in this section represent average values after repeating each experiment 30 times. 95% confidence intervals obtained were small and have been omitted in the figures shown for clarity.

6.1.1. Coverage-limited scenario

Fig. 9 plots the value of the objective function of the solutions found. It is noticeable that the physical bit rate of IEEE 802.11b (11 Mbps) results in higher demand for drones due to the low throughput supported by each AP. It can also be observed that when geographic dispersion increases, standards in the 5 GHz band (IEEE 802.11a and 802.11ac) produce worse results (i.e. more UAVs are needed) than those in the 2.4 GHz band. This can be attributed to a higher propagation loss (see RSSI expressionformula in (5)). Another noticeable effect is produced by the channel bandwidth. Higher bandwidth exhibits higher thermal noise (see N formula in (8)), which negatively impacts SNR and, consequently, coverage. This is clearly noticeable in the case of IEEE 802.11ac, and less obvious in IEEE 802.11n, which performs a little worse than IEEE 802.11 g for areas greater than 70 m×70 m despite a greater data bit rate.

Finally, an interesting effect can be observed in the leftmost part of the figure. Most revisions start with 4 drones and then fall to 3 for larger areas until it starts increasing again. This is attributable to the scenario characteristics as in the denseset case (100 users in an area of 10 m × 10 m) it behaves like a QoS-limited scenario where 100% of users are covered, and the limiting factor is their traffic. However, when the terrain size increases (i.e. sparsity increases) some users are left uncovered (until $C_{\min}$). This happens first in those standard revisions that exhibit worse coverage properties (i.e. ac and a), and as a consequence, fewer drones are required. Nevertheless, as the terrain size keeps increasing, coverage constraint is dominant, and the number of drones in the solutions tends to increase with the terrain size in all standard revisions but IEEE 802.11b due to the large number of drones deployed.

6.1.2. QoS-limited scenario

Fig. 10 shows the results obtained for the high user-density QoS-limited scenario. To be consistent with the previous case, we consider user sparsity ($0,25$–1 m^2/user) instead of density in the results shown. Results show that all standard revisions (but IEEE 802.11b) exhibit similar behavior, increasing the number of drones when QoS constraints

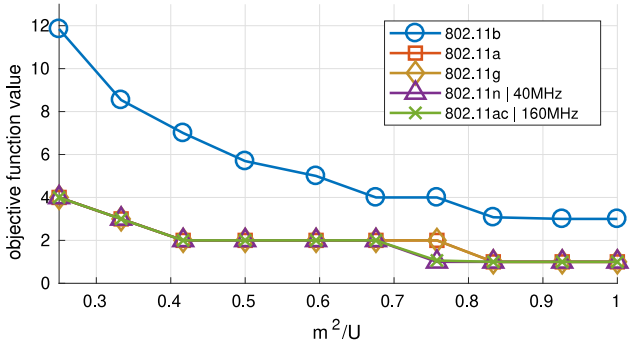

Fig. 10. QoS limited scenario.

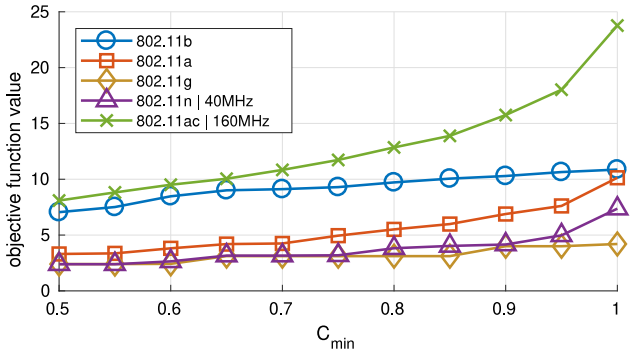

Fig. 11. Influence of $C_{\min}$ in the value of the objective function.

are not met due to high traffic volume. This suggests that the higher data bit rate exhibited by some revisions is not fully exploited (except at 0.76 m^2/user) in the very small scenario under consideration. As expected, the insufficient physical bit-rate of IEEE 802.11b causes exponential growth in the number of drones required to support very high user densities.

From the two scenarios studied, it can be concluded that revisions IEEE 802.11 g/n achieve the best results, requiring only between 1 and 4 drones to cover between 90 and 100 users in an area ranging from 5 m × 5 m up to 100 m × 100 m. Revisions using 5 GHz however (a, ac), exhibit more path loss and tend to require more drones in large areas e.g. greater than 70 ×70 m. Finally, the old IEEE 802.11b standard revision exhibits a poor performance compared with the rest as a result of its poor throughput.

6.2. Influence of the constraints

The selection of the constraints' thresholds also plays an important role in the solutions obtained; very restrictive constraints may lead to unwanted results. In this section, we show the results produced with the variation of $C_{\min}$ in a *coverage-limited* scenario (100 users in the largest terrain size: 10 000 m^2), and $B_{\max}$ in a *QoS-limited* scenario (100 users in the smallest terrain size: 25 m^2). The value of MOS_{min} is always set to 3.5.

Fig. 11 shows the influence of $C_{\min}$ in the objective function for different IEEE 802.11 standard revisions. As expected, the number of drones in the solutions increases with $C_{\min}$. This growth is approximately linear until $C_{\min} = 0.9$, where those standard revisions with higher frequency (a, ac) or channel bandwidth (ac, n) exhibit a steeper rise than b or g. Therefore, very demanding $C_{\min}$ values may cause exponential growth in the number of UAVs needed for those standards. In such case, the maximum number of available UAVs in the problem ($D_{\max}$) might limit the feasibility of finding valid solutions.

Fig. 12 shows the influence of $B_{\max}$ in the objective function for a very small area with a highly dense crowd. Recall that $B_{\max} = 0$ means

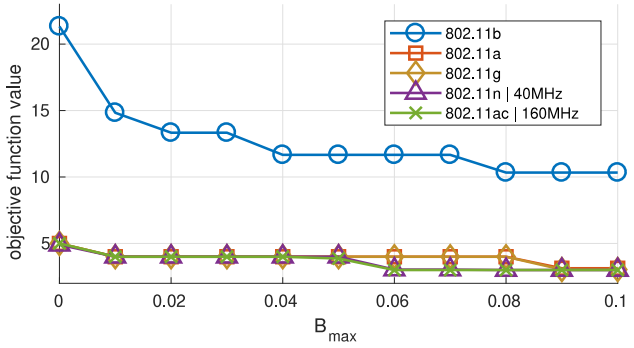

Fig. 12. Influence of $B_{\max}$ in the value of the objective function.

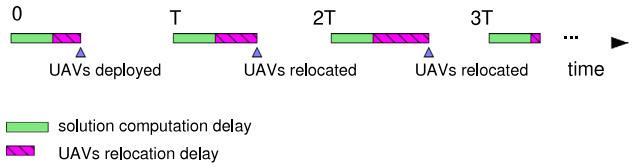

Fig. 13. Dynamic of UAVs relocation.

that all users associated to WiFi (i.e. covered) can simultaneously call, whereas $B_{\max} = 0.1$ means that a covered user will be allowed (by the CAC mechanism) to call with a probability of 90%. In this case, those standards with better data bit rate withstand more restrictive values of $B_{\max}$ (i.e. simultaneous calls) with the same number of drones. As such, we find that IEEE 802.11n/ac revisions achieve slightly better results than the rest.

Finally, it is important to remark that several factors limit our numerical results. First, only the highest data bit rate from each revision has been considered; then, some features such as frame aggregation or MIMO in 802.11n or 802.11ac have also been disregarded, so it has the inter-channel interference. Besides, some promising revisions such as IEEE 802.11ah, targeted explicitly for outdoor long-range at 900 MHz serving high-density wireless stations [23] has not been included due to lack of adoption in today's user terminals. However, the most patent limit of our results is the fact that the problem has been applied just to the initial deployment of UAVs. Next, we provide a preliminary analysis of the applicability of this problem to a scenario where ground users are moving.

7. Application to moving targets

The problem defined in Eq. (3) is aimed at solving the problem of the initial deployment of UAVs, and as such, it can also be applied for service provisioning when ground users are gathered in specific known areas such as meeting points. In this section, we provide a brief analysis of its applicability when ground users are on the move, identifying open issues which remain to be addressed in future work. It is assumed that ground users position can be tracked. In such case, every T seconds user's position is updated and our optimization problem is solved, relocating UAVs accordingly in a process like the one illustrated in Fig. 13.

The key points in this process are:

- The observation period T. The minimum possible value for T should be greater than the addition of:
  - The time required to solve the problem (which in turn depends on the performance of the algorithm finally implemented, the scenario under consideration and computational resources).
  - The time required to relocate all UAVs according to the new solution. This, in turn, depends on the solution found, initial position, UAV speed and the displacement strategy.

  Practical values should be in the order of seconds. Clearly, the longer T, the greater discrepancy between the theoretical and actual position of ground users, increasing the error of the models and chances of unsatisfying constraints.
- Relocation of UAVs. Moving UAVs may result in transient periods of unsatisfied constraints. The decision about which drones are displaced according to the final solution and the trajectories followed is a problem itself that should consider not only the delay (e.g.[11]) but also service disruption to ground users engaged in conversations. Examples of strategies include minimizing the sum of all UAVs displacements, the longest UAV displacement, or the number of users affected by service outages. It would also be interesting to explore techniques of machine learning such as conceptor-based echo state networks (ESN) [51] to predict user service request pattern and user mobility pattern.
- Problem Objective function. Once the relocation strategy is fixed, the cost of relocating drones should be considered in the optimization problem as a penalty factor added to the objective function. Let us imagine a case in which two candidate solutions exhibit the same number of drones and coverage (i.e. a similar value of the objective function) but one solution implies a complex repositioning of all drones while the other implies just a slight change on a single drone. Thus, this penalty could include aspects such as the relocation delay or the temporal effect of impaired users due to drones' relocation, serving as a factor to break the deadlock in favor of the less costly solution.

The aforementioned key points suggest that user's movement brings out new issues and implications that require an extension to the problem defined in this paper, including the cost of UAVs relocation according to a specific strategy and user mobility models. Furthermore, a centralized approach such as the one suggested for initial deployment might not hold service continuity. These aspects[15] are left as open issues for further research. Nevertheless, as a prospective exercise, we have performed a simulation with users on the move using the coverage-limited scenario and the parameters in Table 4 (but using a traffic profile of 5 calls/hour/user and altitude layers between 10 m and 40 m with steps of 1 m).

In our coverage-limited scenario, the 100 users now move according to a correlated random walk model. Each ground user moves at a walking speed of 5.3 km/h with a probability of 0.8, and in such case, the direction remains unchanged with a probability of 0.8. Users rotate 180 degrees when they reach the area bounds. Algorithm 3 is used for the initial deployment and the number of drones deployed D remains unchanged for the remainder of the simulation (30 min). To achieve this, we limit subsequent solutions to the best possible found by our GA with D drones (even though problem constraints were not satisfied). With every new solution, drones are relocated (considering a speed of 60 Km/h) so that the sum of the distances traveled by all drones is the minimum possible.

To study the transient effects of UAV relocation, we check every five seconds whether the problem constraints (i.e. coverage and speech quality) are satisfied considering the actual position of users. New solutions (and drones relocation) have been recalculated every $T = \{15\,\text{s}, 30\,\text{s}, 45\,\text{s}, 60\,\text{s}\}$ and in each case simulations are repeated 30 times. Fig. 14 shows the percentage of the simulation time when both constraints are satisfied. Results show that problem constraints were satisfied above 92% of the time in the worst case (i.e. area of 10 000 m^2 and $T = 60$ s). As expected, the worse performance is obtained when users are more scattered and, to a lesser extent, with longer T.

[15] Another open issue is to speed up the solution search by experimenting with other heuristics or at the implementation level (e.g. using low-level programming language).

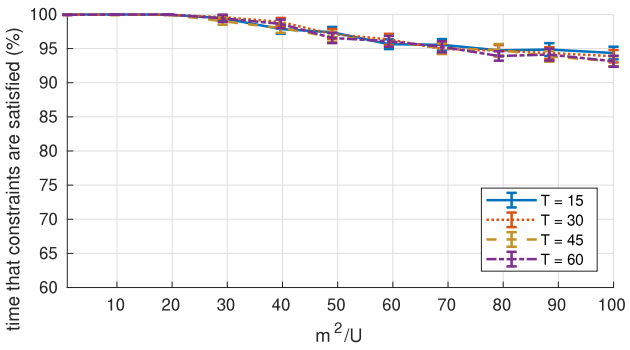

Fig. 14. Effect of UAV relocation in problem constraints.

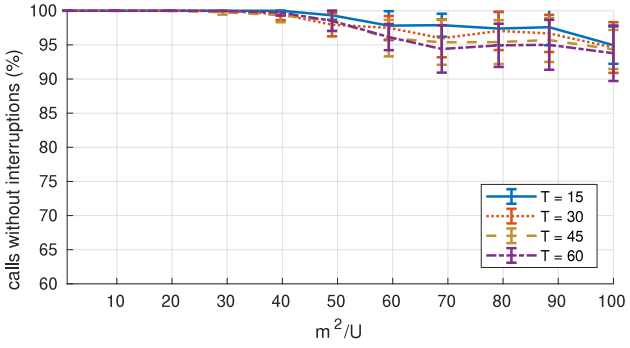

Fig. 15. Effect of UAV relocation in calls in progress.

But since users call according to a traffic profile of 5 calls/hour, it would be interesting to observe the impairment that drones relocation cause in these calls. To this end, we define a call disruption event when a call in progress does not satisfy the speech quality constraint for two consecutive samples (i.e. 10 s). The percentage of calls that experience a service free of disruption is shown in Fig. 15. According to our results, after the 30 min of simulation, almost 95% of calls have not been affected by disruption events. As in the previous case, results show a slight decrease for larger scenarios with more scattered users and to a lesser extent with T.

A final experiment was done by launching one extra drone ($D+1$) in the initial deployment (i.e. forcing one extra iteration in Algorithm 3). The results obtained in this case were promising since the effect of UAV relocation was unnoticed (i.e. constraints were met 100% of the time, and no call was interrupted). This suggests that launching extra drones[16] can be an effective method to avoid service degradation during UAVs relocation.

8. Conclusions and further work

In this paper, we dealt with the problem of optimal placement of UAVs to provide a VoWiFi service with guaranteed QoS to a set of static users. We formulated an optimization problem that minimizes the number of drones required to provide such service and the ratio of uncovered users. An exhaustive search algorithm was proposed to find solutions. Still, due to its high computational cost, we also proposed efficient heuristics as a general way to solve the optimization problem.

The results obtained in our experiments suggest that large area scenarios with highly dispersed users (coverage-limited) will benefit from IEEE 802.11 g/n standards, as fewer drones will be needed to provide the service. However, in very small scenarios with a highly dense crowd, the limiting factor will be QoS, and fewer drones will be required by using IEEE 802.11 standards with a higher bit rate.

The next step in our work is to include the energy of the communication and the blocking probability as part of the objective function in a combination customizable by the designer. It is also left for further work the full extension of this problem to ground users on the move exploring relocation strategies and launching extra drones.

[16] Although we used one extra drone, the optimal number will end up depending on users' density and terrain extension, which is also left for further research.

Declaration of competing interest

The authors declare that they have no known competing financial interests or personal relationships that could have appeared to influence the work reported in this paper.

Appendix A. Expected time per slot: E [T]

The expected time per slot represents the expected length of each state of the Markov chain modeling the IEEE 802.11 system. To obtain a closed-form expression of $E[T]$, we follow the approach presented in [35] (but adapted to the terms and concepts defined in Section 4.2) which considers the probability of being on each of the following states:

- Idle state, when nobody attempts to transmit.
- Success state, when only a single station attempts to transmit with no channel related errors.
- Error state, when a single station attempts to transmit but channel errors occur.
- Collision state, when more than one station attempts to transmit simultaneously (same slot).

$E[T]$ can be obtained by weighting the time spent on each of the previous states respectively as follows:

$$E[T] = T_I + T_S + T_E + T_C \tag{A.1}$$

The factors in (A.1) can be calculated as follows:

- T_I can be expressed as:

$$T_I = P_I\ \sigma \tag{A.2}$$

where σ stands for the time slot duration as defined in the corresponding IEEE 802.11 revision. P_I is the probability that the channel is idle in a randomly chosen slot, which can be expressed as

$$P_I = \prod_{j=1}^{S} \left(1 - \tau^{(j)}\right) \tag{A.3}$$

where S is the number of stations in the system under consideration . Let us define this set as $S = \mathcal{M} \cup AP$. Then, $S = |S| = |\mathcal{M}| + 1$.

- The time spent on successful (T_S) and erroneous (T_E) slots can be expressed as:

$$T_S = \sum_{j=1}^{S} P_s^{(j)}\ (1 - \mathrm{FER}^{(j)})\ T_s^{(j)} \tag{A.4}$$

$$T_E = \sum_{j=1}^{S} P_s^{(j)}\ \mathrm{FER}^{(j)}\ T_e^{(j)} \tag{A.5}$$

where $T_s^{(j)}$ and $T_e^{(j)}$ represent the average time that station j spends in successful and erroneous transmissions, respectively. Their actual value depend on the IEEE 802.11 standard revision used and physical data rate of stations. They can be expressed as:

$$T_s^{(j)} = \mathrm{DIFS} + 2 \cdot \mathrm{PLCP}^{(j)} + (\mathrm{Header}^{(j)} + \mathrm{Data}^{(j)})/R_b^{(j)} + \mathrm{SIFS} + T_{ack} + 2\delta \tag{A.6}$$

$$E[T] = \underbrace{\sigma \cdot \prod_{j=1}^{S}\left(1-\tau^{(j)}\right)}_{T_I,} + \underbrace{\sum_{j=1}^{S}\tau^{(j)}\left(\prod_{k=1,\ k\neq j}^{S}\left(1-\tau^{(k)}\right)\right)\left(1-\mathrm{FER}^{(j)}\right)T_s^{(j)}}_{T_S} + \underbrace{\sum_{j=1}^{S}\tau^{(j)}\left(\prod_{k=1,\ k\neq j}^{S}\left(1-\tau^{(k)}\right)\right)\mathrm{FER}^{(j)}\,T_e^{(j)}}_{T_E} +$$

$$\underbrace{\sum_{d=1}^{N_c}\left(\prod_{j\in\mathcal{H}(d)}\left(1-\tau^{(j)}\right)\right)\left(\prod_{j\in\mathcal{L}(d)}\left(1-\tau^{(j)}\right)\right)\left(\left(1-\prod_{j\in\mathcal{N}(d)}\left(1-\tau^{(j)}\right)\right)-\sum_{j\in\mathcal{N}(d)}\left(\tau^{(j)}\prod_{k=1,\ k\neq j}^{S}\left(1-\tau^{(k)}\right)\right)\right)\cdot T_c^{(d)}}_{T_C}$$

$$+\underbrace{\sum_{d=1}^{N_c}\left(1-\prod_{j\in\mathcal{N}(d)}\left(1-\tau^{(j)}\right)\right)\left(1-\prod_{j\in\mathcal{H}(d)}\left(1-\tau^{(j)}\right)\right)\left(1-\left(1-\prod_{j\in\mathcal{L}(d)}\left(1-\tau^{(j)}\right)\right)\right)\cdot T_c^{(d)}}_{T_C\,(\text{continued})} \tag{A.19}$$

Box I.

$$T_e^{(j)} = \mathrm{DIFS} + \mathrm{PLCP}^{(j)} + (\mathrm{Header}^{(j)} + \mathrm{Data}^{(j)})/R_b^{(j)} + \mathrm{EIFS} + \delta \tag{A.7}$$

Where $R_b^{(j)}$ represents the physical data rate (given by the MCS used by the station), DIFS, SIFS, EIFS are inter-frame periods as specified by the 802.11 standard and $\mathrm{PLCP}^{(j)}$, $\mathrm{Header}^{(j)}$ and T_{ack} correspond with the PLCP header, the IEEE 802.11 header and the duration of an *ack* frame in the IEEE 802.11 standard,[17] and δ is the propagation delay.

In Eqs. (A.4) and (A.5), $P_s^{(j)}$ stands for the probability that only an observed station j attempts to transmit while the rest remain silent, which can be expressed as:

$$P_s^{(j)} = \tau^{(j)} \prod_{k=1,\ k\neq j}^{S}\left(1-\tau^{(k)}\right) \tag{A.8}$$

- The time spent in collided transmissions T_C can be deduced as follows. Each station j exhibits an average collision time, $T_c^{(j)}$ which can be approximated by the time spent in a erroneous transmission $T_e^{(j)}$ (i.e. $T_c^{(j)} = T_e^{(j)}$). Nevertheless, when packets sent by two different station collide, the time to be considered corresponds with the longest average collision time. To address this concern, stations in the system (i.e. set $\mathcal{S}$) are grouped in traffic classes according to their collision time (i.e. all stations with the same average collision time belong to the same class). Then, the following subsets of $\mathcal{S}$ can be defined:

$$\underset{i\in 1..S}{\mathcal{N}(i)} = \left\{j \in \mathcal{S} \mid T_c^{(j)} = T_c^{(i)}, j \notin \mathcal{N}(k), k \leq i\right\} \tag{A.9}$$

Where $\mathcal{N}(i)$ is a subset of $\mathcal{S}$ that includes those stations whose collision time is $T_c^{(i)}$ (only if such stations are not yet in other group $\mathcal{N}(j)$ with $j < i$). Notice that (A.9) defines multiple groups (e.g. $\mathcal{N}(1), \mathcal{N}(2), \ldots, \mathcal{N}(S)$), and since each station can only belong to one group (or class), some of the previous classes may be empty sets. Therefore, let us define a new set which can be used to identify non-empty sets as:

$$\mathcal{E} = \left\{i \mid \mathcal{N}(i) \neq \varnothing\right\} \tag{A.10}$$

The number of non-empty classes will be finally given by $N_c = |\mathcal{E}|$.

Considering $\mathcal{N}(d)$ as the set of stations that belong to class $d \in \mathcal{E}$, let us define $\mathcal{L}(d)$ as the set of stations whose collision time is longer than $T_c^{(d)}$ (i.e. their data bit rate is slower), and $\mathcal{H}(d)$ as the set of stations whose collision time is shorter than $T_c^{(d)}$ (i.e. their data bit rate is faster). $\mathcal{H}(d)$ and $\mathcal{L}(d)$ can be formally defined as:

$$\mathcal{L}(d) = \left\{i \in \mathcal{S} \mid T_c^{(i)} > T_c^{(d)}\right\} \tag{A.11}$$

$$\mathcal{H}(d) = \left\{i \in \mathcal{S} \mid T_c^{(i)} < T_c^{(d)}\right\} \tag{A.12}$$

Now the probability that at least one station that belongs to class $d \in \mathcal{E}$ transmits is:

$$P_{tx}^{\mathcal{N}(d)} = 1 - \prod_{j\in\mathcal{N}(d)}\left(1-\tau^{(j)}\right) \tag{A.13}$$

And the probabilities that at least one station from a higher or lower class transmits are:

$$P_{tx}^{\mathcal{H}(d)} = 1 - \prod_{j\in\mathcal{H}(d)}\left(1-\tau^{(j)}\right) \tag{A.14}$$

$$P_{tx}^{\mathcal{L}(d)} = 1 - \prod_{j\in\mathcal{L}(d)}\left(1-\tau^{(j)}\right) \tag{A.15}$$

Due to the fact that lower classes slow down higher ones as a result of longer transmission times, T_C can be calculated as:

$$T_C = \sum_{d=1}^{N_c}\left(P_c^{\mathcal{N}(d)} + P_c^{\mathcal{H}(d)}\right)T_c^{(d)} \tag{A.16}$$

where $T_c^{(d)}$ is the average time that any station from class d spends on collision state, and $P_c^{\mathcal{N}(d)}$ represents the probability that any collision occurs between stations from the same class d:

$$P_c^{\mathcal{N}(d)} = \left(1-P_{tx}^{\mathcal{H}(d)}\right)\cdot\left(1-P_{tx}^{\mathcal{L}(d)}\right)\cdot\left(P_{tx}^{\mathcal{N}(d)} - \sum_{j\in\mathcal{N}(d)}P_s^{(j)}\right) \tag{A.17}$$

and $P_c^{\mathcal{H}(d)}$ accounts for the probability that class d is involved in a collision with at least one station from a higher class.

$$P_c^{\mathcal{H}(d)} = P_{tx}^{\mathcal{N}(d)}\cdot P_{tx}^{\mathcal{H}(d)}\cdot\left(1-P_{tx}^{\mathcal{L}(d)}\right) \tag{A.18}$$

Finally, substituting the expressions of T_I, T_S, T_E, and T_C in (A.1), the closed-form expression of $E[T]$ presented in (A.19) (see Box I) is obtained.

Appendix B. Raw fitness criteria evaluation

Assessing *raw fitness scores* entails solving both signal coverage (e.g. RSSI and SNR) and the analytical models to estimate QoS. This appendix provides a pseudocode in Algorithm 4 that can be used as a guidance for implementation and also to estimate the computational complexity of this step.

The algorithm can be divided in the following parts:

[17] Note that in the AP station these times are averaged considering the physical data rate and/or codec of every user in $\mathcal{M}$.

- Lines 1–6: RSSI and SNR are calculated for each pair ground user–drone.
- Lines 7–15: Each ground user station is associated to a specific drone, creating $\mathcal{C}(i)$.
- Lines 19–24: The maximum number of concurrent calls $CC_{\max}$ is calculated for each drone k, which depends on the blocking probability constraint $B_{\max}$.
- Lines 25: The set of stations $S = \mathcal{M} \cup AP$, is created selecting the $CC_{\max}$ slowest ground users stations and the AP.
- Lines 26–42: The non-linear equation system is solved iteratively, the output is the estimation of the MOS experienced by users associated to drone k.

Input: $\mathcal{U} = \{1, \ldots, U\}$, $D = \{1, \ldots, D\}$, $\{\boldsymbol{w}_i \mid i \in \mathcal{U}\}$, $\{\boldsymbol{x}_k \mid k \in D\}$
Initialization: $f_{\text{fitness}} = D + 2$
Output: f_{fitness}

1 **for** $i = 1$ **to** U **do**
2 **for** $j = 1$ **to** D **do**
3 *calculate* $\text{RSSI}_{i,j}$; // Eq. (5)
4 *calculate* $\text{SNR}_{i,j}$; // Eq. (7)
5 **end**
6 **end**
7 **for** $i = 1$ **to** U **do**
8 **for** $k = 1$ **to** D **do**
9 **if** $RSSI_{i,k} \geq RSSI_{\min}$ ***and*** $SNR_{i,k} \geq SNR_{\min}$ **then**
10 **if** $RSSI_{i,k} > RSSI_{i,j},\ \forall j \neq k$ **then**
11 $C(k) = C(k) \cup i$;
12 **end**
13 **end**
14 **end**
15 **end**
16 **if** $\sum_{i=1}^{D} |C(i)|/U \geq C_{\min}$ **then**
17 **for** $k = 1$ **to** D **do**
18 *calculate* $CC_{\max}$; // Algorithm 2
19 *build set* $S = \mathcal{M} \cup \mathcal{AP}$;
20 **for** $j = 1$ **to** $|S|$ **do**
21 *calculate* $T_s^{(j)}$, $T_c^{(j)}$, $T_e^{(j)}$;
22 *calculate* $\text{FER}^{(j)}$; // Eq. (17)
23 **end**
24 $\tau_{\text{next}}^{(j)} = T_c^{(j)},\ \forall j$;
25 **while** *diff* $> \Delta$ **do**
26 $\tau^{(j)} = \tau_{\text{next}}^{(j)}$;
27 *calculate* $E[T]$; // Appendix Appendix A
28 **for** $j = 1$ **to** $|S|$ **do**
29 *calculate* $E[B^{(j)}]$; // Eq. (13)
30 *calculate* $r^{(j)}$, $q^{(j)}$; // Eqs. (11), (12)
31 *calculate* $p^{(j)}$; // Eq. (15)
32 *calculate* $\tau_{\text{next}}^{(j)}$; // Eq. (10)
33 **end**
34 $diff = \max\left(|\tau_{\text{next}}^{(j)} - \tau^{(j)}|\right),\ \forall j$;
35 **end**
36 *calculate* $\text{MOS}(k)$; // Eq. (25)
37 **end**
38 **if** $MOS(k) \geq MOS_{\min},\ \forall k \in \{1, \ldots, D\}$ **then**
39 $f_{\text{fitness}} = D + \left(1 - \sum_{k=1}^{D} |C(k)|/U\right)$;
40 **else**
41 $f_{\text{fitness}} = D + 1 + \left(1 - \sum_{k=1}^{D} |C(k)| \left[\text{MOS}(k) < \text{MOS}_{\min}\right]/U\right)$;
42 **end**
43 **end**

Algorithm 4: Fitness function evaluation

References

[1] R. Clarke, Understanding the drone epidemic, Comput. Law Secur. Rev. 30 (3) (2014) 230–246.
[2] Y. Zeng, R. Zhang, T.J. Lim, Wireless communications with unmanned aerial vehicles: opportunities and challenges, IEEE Commun. Mag. 54 (5) (2016) 36–42, http://dx.doi.org/10.1109/MCOM.2016.7470933.
[3] I. Jawhar, N. Mohamed, J. Al-Jaroodi, D.P. Agrawal, S. Zhang, Communication and networking of UAV-based systems: Classification and associated architectures, J. Netw. Comput. Appl. 84 (2017) 93–108.
[4] A. Hayajneh, S. Zaidi, D.C. McLernon, M. Di Renzo, M. Ghogho, Performance analysis of UAV enabled disaster recovery networks: A stochastic geometric framework based on cluster processes, IEEE Access (2018).
[5] M. Erdelj, M. Król, E. Natalizio, Wireless sensor networks and multi-UAV systems for natural disaster management, Comput. Netw. 124 (2017) 72–86.
[6] M.S. Alvissalim, B. Zaman, Z.A. Hafizh, M.A. Ma'sum, G. Jati, W. Jatmiko, P. Mursanto, Swarm quadrotor robots for telecommunication network coverage area expansion in disaster area, in: SICE Annual Conference (SICE), 2012 Proceedings of, IEEE, 2012, pp. 2256–2261.
[7] M. Deruyck, J. Wyckmans, L. Martens, W. Joseph, Emergency ad-hoc networks by using drone mounted base stations for a disaster scenario, in: Wireless and Mobile Computing, Networking and Communications (WiMob), 2016 IEEE 12th International Conference on, IEEE, 2016, pp. 1–7.
[8] G. Tuna, B. Nefzi, G. Conte, Unmanned aerial vehicle-aided communications system for disaster recovery, J. Netw. Comput. Appl. 41 (2014) 27–36.
[9] Y. Li, L. Cai, UAV-assisted dynamic coverage in a heterogeneous cellular system, IEEE Netw. 31 (4) (2017) 56–61.
[10] D. Zorbas, L.D.P. Pugliese, T. Razafindralambo, F. Guerriero, Optimal drone placement and cost-efficient target coverage, J. Netw. Comput. Appl. 75 (2016) 16–31.
[11] X. Zhang, L. Duan, Fast deployment of UAV networks for optimal wireless coverage, IEEE Trans. Mob. Comput. 18 (3) (2019) 588–601, http://dx.doi.org/10.1109/TMC.2018.2840143.
[12] A. Malik, J. Qadir, B. Ahmad, K.-L.A. Yau, U. Ullah, QoS in IEEE 802.11-based wireless networks: A contemporary review, J. Netw. Comput. Appl. 55 (2015) 24–46, http://dx.doi.org/10.1016/j.jnca.2015.04.016, URL http://www.sciencedirect.com/science/article/pii/S1084804515000892.
[13] L.X. Cai, X. Shen, J.W. Mark, L. Cai, Y. Xiao, Voice capacity analysis of WLAN with unbalanced traffic, IEEE Trans. Veh. Technol. 55 (3) (2006) 752–761, http://dx.doi.org/10.1109/TVT.2006.874145.
[14] E. Charfi, L. Chaari, L. Kamoun, New adaptive frame aggregation call admission control (AFA-CAC) for high throughput WLANs, Trans. Emerg. Telecommun. Technol. 26 (3) (2015) 469–481.
[15] H.-T. Wu, M.-H. Yang, K.-W. Ke, The design of QoS provisioning mechanisms for wireless networks, in: Pervasive Computing and Communications Workshops (PERCOM Workshops), 2010 8th IEEE International Conference on, IEEE, 2010, pp. 756–759.
[16] S. Shin, H. Schulzrinne, Measurement and analysis of the VoIP capacity in IEEE 802.11 WLAN, IEEE Trans. Mob. Comput. (9) (2009) 1265–1279.
[17] E. Yanmaz, R. Kuschnig, C. Bettstetter, Achieving air-ground communications in 802.11 networks with three-dimensional aerial mobility, in: INFOCOM, 2013 Proceedings IEEE, IEEE, 2013, pp. 120–124.
[18] C.-M. Cheng, P.-H. Hsiao, H. Kung, D. Vlah, Performance measurement of 802.11 a wireless links from UAV to ground nodes with various antenna orientations, in: Computer Communications and Networks, 2006. ICCCN 2006. Proceedings. 15th International Conference on, IEEE, 2006, pp. 303–308.
[19] W. Kim, T. Song, T. Kim, H. Park, S. Pack, VoIP capacity analysis in full duplex WLANs, IEEE Trans. Veh. Technol. 66 (12) (2017) 11419–11424, http://dx.doi.org/10.1109/TVT.2017.2729590.
[20] G. Bianchi, Performance analysis of the IEEE 802.11 distributed coordination function, IEEE J. Sel. Areas Commun. 18 (3) (2000) 535–547.
[21] A. Kumar, E. Altman, D. Miorandi, M. Goyal, New insights from a fixed-point analysis of single cell IEEE 802.11 WLANs, IEEE/ACM Trans. Netw. 15 (3) (2007) 588–601.
[22] S. Morgenthaler, T. Braun, Z. Zhao, T. Staub, M. Anwander, UAVNet: A mobile wireless mesh network using unmanned aerial vehicles, in: Globecom Workshops (GC Wkshps), 2012 IEEE, IEEE, 2012, pp. 1603–1608.
[23] S. Aust, R.V. Prasad, I.G. Niemegeers, Outdoor long-range WLANs: a lesson for IEEE 802.11 ah, IEEE Commun. Surv. Tutor. 17 (3) (2015) 1761–1775.
[24] J.A. Bergstra, C.A. Middelburg, ITU-T Recommendation P.800 : Methods for Subjective Determination of Transmission Quality, Tech. Rep., 1996.
[25] S. Karapantazis, F.-N. Pavlidou, VoIP: A comprehensive survey on a promising technology, Comput. Netw. 53 (12) (2009) 2050–2090, http://dx.doi.org/10.1016/j.comnet.2009.03.010, URL http://www.sciencedirect.com/science/article/pii/S1389128609001200.
[26] A. Chhabra, D. Singh, Assessment of VoIP E-model over 802.11 wireless mesh network, in: 2015 International Conference on Advances in Computer Engineering and Applications, 2015, pp. 856–860, http://dx.doi.org/10.1109/ICACEA.2015.7164824.

[27] ITU-T Recommendation G.107 : The E-Model, a Computational Model for Use in Transmission Planning, Tech. Rep., International Telecommunication Union, 2015.
[28] T. Triyason, P. Kanthamanon, E-model modification for multi-languages over IP, Elektronika Ir Elektrotechnika 21 (1) (2015) 82–87.
[29] H. Assem, D. Malone, J. Dunne, P. O'Sullivan, Monitoring VoIP call quality using improved simplified E-model, in: Computing, Networking and Communications (ICNC), 2013 International Conference on, IEEE, 2013, pp. 927–931.
[30] R.G. Cole, J.H. Rosenbluth, Voice over IP performance monitoring, ACM SIGCOMM Comput. Commun. Rev. 31 (2) (2001) 9–24.
[31] J. Janssen, D. De Vleeschauwer, M. Buchli, G.H. Petit, Assessing voice quality in packet-based telephony, IEEE Internet Comput. 6 (3) (2002) 48–56.
[32] IEEE standard for information technology–telecommunications and information exchange between systems local and metropolitan area networks–specific requirements - Part 11: Wireless LAN medium access control (MAC) and physical layer (PHY) specifications, in: IEEE Std 802.11-2016, Revision of IEEE Std 802.11-2012, 2016, pp. 1–3534, http://dx.doi.org/10.1109/IEEESTD.2016.7786995.
[33] K. Duffy, A.J. Ganesh, Modeling the impact of buffering on 802.11, IEEE Commun. Lett. 11 (2) (2007).
[34] D. Malone, K. Duffy, D. Leith, Modeling the 802.11 distributed coordination function in nonsaturated heterogeneous conditions, IEEE/ACM Trans. Netw. 15 (1) (2007) 159–172.
[35] M. Laddomada, F. Mesiti, M. Mondin, F. Daneshgaran, On the throughput performance of multirate IEEE 802.11 networks with variable-loaded stations: analysis, modeling, and a novel proportional fairness criterion, IEEE Trans. Wireless Commun. 9 (5) (2010).
[36] K.R. Duffy, Mean field Markov models of wireless local area networks, Markov Process. Related Fields 16 (2) (2010) 295–328.
[37] E.W. Wong, A. Zalesky, M. Zukerman, On generalizations of the Engset model, IEEE Commun. Lett. 11 (4) (2007).
[38] M. Mozaffari, W. Saad, M. Bennis, M. Debbah, Drone small cells in the clouds: Design, deployment and performance analysis, in: 2015 IEEE Global Communications Conference, GLOBECOM, 2015, pp. 1–6, http://dx.doi.org/10.1109/GLOCOM.2015.7417609.
[39] P. Yang, X. Cao, X. Xi, Z. Xiao, D. Wu, Three-dimensional drone-cell deployment for congestion mitigation in cellular networks, IEEE Trans. Veh. Technol. 67 (10) (2018) 9867–9881, http://dx.doi.org/10.1109/TVT.2018.2857211.
[40] A. Al-Hourani, S. Kandeepan, S. Lardner, Optimal LAP altitude for maximum coverage, IEEE Wirel. Commun. Lett. 3 (6) (2014) 569–572, http://dx.doi.org/10.1109/LWC.2014.2342736.
[41] N.C. Taher, Y. Ghamri-Doudane, B. El Hassan, N. Agoulmine, An efficient model-based admission control algorithm to support voice and video services in 802.11 e WLANs, in: Information Infrastructure Symposium, 2009. GIIS'09. Global, IEEE, 2009, pp. 1–8.
[42] J. Zhu, A.O. Fapojuwo, A new call admission control method for providing desired throughput and delay performance in IEEE802. 11e wireless LANs, IEEE Trans. Wireless Commun. 6 (2) (2007).
[43] D. Pong, T. Moors, Call admission control for IEEE 802.11 contention access mechanism, in: Global Telecommunications Conference, 2003. GLOBECOM'03. IEEE, Vol. 1, IEEE, 2003, pp. 174–178.
[44] Q. Zhao, D.H. Tsang, T. Sakurai, Modeling nonsaturated IEEE 802.11 DCF networks utilizing an arbitrary buffer size, IEEE Trans. Mob. Comput. 10 (9) (2011) 1248–1263.
[45] G. Pei, T.R. Henderson, Validation of Ns-3 802.11b PHY Model, Tech. Rep., Boeing Research and Technology, 2009.
[46] T.R.H. Guangyu Pei, Validation of OFDM Error Rate Model in Ns-3, Tech. Rep., Boeing Research and Technology, 2010.
[47] A. Chipperfield, P. Flemming, H. Pohlheim, C. Fonseca, Genetic algorithm toolbox for use with MATLAB, 1994.
[48] H.E. Aguirre, K. Tanaka, T. Sugimura, Cooperative model for genetic operators to improve GAs, in: Proceedings 1999 International Conference on Information Intelligence and Systems, Cat. No.PR00446, 1999, pp. 98–106, http://dx.doi.org/10.1109/ICIIS.1999.810230.
[49] H.E. Aguirre, K. Tanaka, T. Sugimura, S. Oshita, Improved distributed genetic algorithm with cooperative-competitive genetic operators, in: Smc 2000 Conference Proceedings. 2000 Ieee International Conference on Systems, Man and Cybernetics. 'Cybernetics Evolving to Systems, Humans, Organizations, and their Complex Interactions', Vol. 5, Cat. No.0, 2000, pp. 3816–3822, http://dx.doi.org/10.1109/ICSMC.2000.886605.
[50] B. Dengiz, F. Altiparmak, A.E. Smith, Local search genetic algorithm for optimal design of reliable networks, IEEE Trans. Evol. Comput. 1 (3) (1997) 179–188, http://dx.doi.org/10.1109/4235.661548.
[51] M. Chen, M. Mozaffari, W. Saad, C. Yin, M. Debbah, C.S. Hong, Caching in the sky: Proactive deployment of cache-enabled unmanned aerial vehicles for optimized quality-of-experience, IEEE J. Sel. Areas Commun. 35 (5) (2017) 1046–1061, http://dx.doi.org/10.1109/JSAC.2017.2680898.